Solar Energetic Particles in the Inner Heliosphere

Author: Mariona Adillón Corbera

Advisor: Neus Agueda Costafreda

Facultat de Física, Universitat de Barcelona, Diagonal 645, 08028 Barcelona, Spain.

Abstract: The upcoming missions *Solar Orbiter* (*SolO*) and *Solar Probe Plus* (*SPP*) will explore the inner region of the heliosphere. To understand the environment in which these missions will operate, we studied the main characteristics of the Interplanetary Magnetic Field (IMF). The IMF can be described by an Archimedean spiral whose curvature is more pronounced for small values of the solar wind speed. In the inner heliosphere ($r < 0.3$ AU), the IMF can be described by a radial magnetic field. At 0.05 AU (*SPP* perihelia), the angle between the magnetic field vector and the radial direction is of only $\psi \simeq 3°$ for a solar wind speed of 400 km/s. Under the assumption of particle scatter-free transport along the IMF, we studied the degree of anisotropy expected at different radial distances from the Sun and how this depends on the location where the particle release occurred. We obtained that the particle pitch angle, α, decreases with radial distance and the decrease is faster for inner source locations. Then the distribution is more beamed for inner source positions and for positions of the observer further out from the Sun. In addition, the study of the particle equation of motion shows that for a fixed distance along the field line particles coming from different source positions reach the observer at different times. Particles released closer to the Sun will arrive later to the same observer. Finally, we analyzed the focusing cone expected in different regions of the heliosphere due to different source positions. We found broader PADs in the inner heliosphere and for more external sources, because these particles suffer less focusing.

I. INTRODUCTION

We live in the extended atmosphere of the Sun, the heliosphere. Events on the Sun drive the fundamental physics of the heliosphere, magnetosphere of the Earth and other planets, affecting satellite communications, power grids, pipelines, radiations exposure on airline flights and astronaut safety. Thus the physics of the solar corona and heliosphere connect the activity of the Sun to environment and technological infrastructure at the Earth.

Solar Energetic Particles (SEPs) are free charged particles emitted by the Sun. They consist of protons, electrons and heavy ions with energies from a few keV to some GeV. They are observed in association with solar eruptive events, such as solar flares or coronal mass ejections (CMEs) [1]. These two phenomena can accelerate charged particles to high energies. Some of these particles escape from the Sun and become observable by spacecraft in the heliosphere. We detect these events at 1 AU by observing an increase in the flux of particles that reach the Earth [2].

A large body of observations in the 1980s led to the formulation of a standard model, by which SEP events are divided into two categories: gradual and impulsive [3]. Gradual events are accelerated at shocks driven by fast CMEs. Impulsive events, on the other hand, are generally ascribed to particle acceleration at sites associated with flares, following magnetic reconnection. The two types of events differ in their typical sizes (with gradual events yielding much larger particle intensities) and in the spatial distribution of their source regions (with impulsive events originating from a comparatively narrow range of solar longitudes that are magnetically well connected to the observer).

Particle motion along a prescribed magnetic field is normally separated in two parts: gyration perpendicular to and translation along the magnetic field direction. The motion of the guiding center can be interpreted as the effective motion of the particle averaged over many gyrations. The particle pitch-angle cosine, μ, is defined as the cosine of the angle between the particle velocity and the magnetic field vector. It is given by

$$\mu = \cos\alpha = \frac{v_{||}}{v} \tag{1}$$

where α is the pitch angle, v is the particle speed and $v_{||}$ is the velocity component parallel to the magnetic field. If v is constant, μ reflects the proportion of particle kinetic energy that corresponds to translation along the interplanetary magnetic field (IMF).

In the absence of large-scale disturbances such as CMEs and shocks, the IMF can be described as a smooth average field, represented by an Archimedean spiral [4]. The magnetic field lines take this shape due to the fact that the field is frozen into the expanding solar wind plasma and the Sun rotates. In this field the first adiabatic invariant remains constant, which is given by

$$\frac{(\sin\alpha)^2}{B} = \text{constant} \tag{2}$$

where B is the field strength.

Note that as particles move along the field into regions of smaller field magnitude, the particle pitch angle decreases, that is the particle motion becomes more focused in the field direction.

The observed particle angular distributions relative to the local direction of the magnetic field (i.e. pitch-angle distributions, PADs) show that particles with pitch angles around 0° (or 180° depending on the IMF polarity)

are the first arriving particles. Under the approximation that particles of different energies are released simultaneously at the Sun, the length of the magnetic field line and the solar release time of the first particles arriving at the spacecraft can be estimated with a direct data analysis method known as velocity dispersion analysis [2]. Particle transport is scatter-free (in contrast to diffusive transport) if the propagation occurs in a smooth magnetic field where field fluctuations can be neglected. The scatter-free regime extends up to 0.5 AU from the Sun [5].

Solar Orbiter (*SolO*) is a mission of the European Space Agency (ESA) planned to launch in October 2018. This mission will make it possible, for the first time, to study the Sun using a combination of in-situ and remote-sensing instruments from as close as 0.28 AU [6]. One of the goals of *SolO* is to identify the origins and causes of SEPs and answer top level science questions like how do solar transient drive heliosphere variability and how do solar eruptions produce energetic particle radiation that fill the heliosphere.

Another similar mission is *Solar Probe Plus* (*SPP*). The spacecraft is planned to be launched in July 2018. *SPP* is a NASA mission and it will be the first mission flying into the low solar corona. *SPP* will sample the solar corona in order to describe how it is heated, and the solar wind and SEPs are accelerated. It will explore the inner region of the heliosphere through in-situ and remote sensing observations of the magnetic field, plasma and energetic particles from 0.05 AU to 0.25 AU [7].

In Section 2 we analyze the main characteristics of the scatter-free particle transport along the IMF in order to understand the environment in which missions such as *SolO* and *SPP* will operate. In Section 3 we study the focusing cone produced by a moving particle source. Finally Section 4 summarizes the main conclusions of the work and the utility of these techniques to interpret the observations that the upcoming missions *SolO* and *SPP* will perform.

II. CHARACTERIZATION OF THE INNER HELIOSPHERE

A. Interplanetary magnetic field: the Archimedean spiral

The strength of the IMF, B, is given by

$$B(r) = B_0 \left(\frac{r_0}{r}\right)^2 \sqrt{1 + \left(\frac{r}{a}\right)^2} \qquad (3)$$

where r_0 is the radius at which the magnetic field is completely frozen into the solar wind, $B_0 = B(r_0)$, and $a = \frac{u}{\Omega}$ where u is the solar wind speed and Ω is the siderial solar rotation rate [8].

Eq. 3 shows how the magnetic field changes as a function of the radial distance. Close to the Sun ($r/a \ll 1$), $B(r) \propto 1/r^2$, while in the outer heliosphere ($r/a \gg 1$),
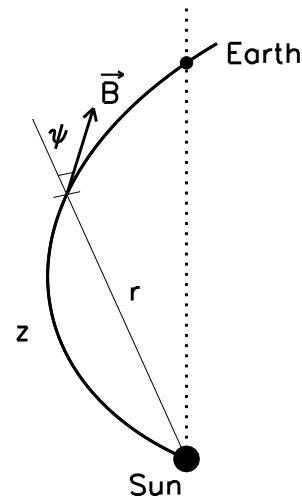

FIG. 1: Archimedean magnetic field line in the ecliptic plane connecting the Sun and the Earth. The length of the field line, z, at a given radial distance, r, and the angle, ψ, between the local magnetic field direction and the radial direction are shown (see text for details).

$B(r) \propto 1/r$, which means that close to the Sun the magnetic field intensity decreases faster.

The large scale configuration of the IMF has a spiral structure (see Fig. 1). The angle, ψ, between the magnetic field vector and the direction of the radius vector from the Sun is given by

$$\sec\psi(r) = \sqrt{1 + \frac{r^2}{a^2}} \qquad (4)$$

which is the same as

$$\tan\psi = \frac{r\Omega}{u} \qquad (5)$$

Thus the angle ψ increases with radial distance from the Sun (the field line becomes more curved) and close to the Sun the magnetic field lines follow a radial direction. In addition, we expect less curved spirals for large values of the solar wind speed. Fig. 2 (top panel) shows the ψ angle for several common values of the solar wind speed from 300 km/s to 500 km/s. At 1 AU we expect ψ to be close to 45° for a solar wind speed of 400 km/s. Closer to the Sun, for example, at 0.05 AU (*SSP* perihelia) or 0.30 AU (*SolO* perihelia), $\psi \simeq 3°$ and $\psi \simeq 18°$, respectively.

A similar behavior is seen by comparing the length of the field line, z, at different radial distances, r, from the Sun. The length of a field line is the integral of the differential distance $dz = \sec\psi dr$ which is given by

$$z(r) = \frac{a}{2}\left[\ln\left(\sqrt{1 + \frac{r^2}{a^2}} + \frac{r}{a}\right) + \frac{r}{a} + \frac{r}{a}\sqrt{1 + \frac{r^2}{a^2}}\right] \quad (6)$$

Fig. 2 (bottom panel) shows the distance z along the field line depending on the radial distance from the Sun. The vertical dashed lines show the outer boundary of the
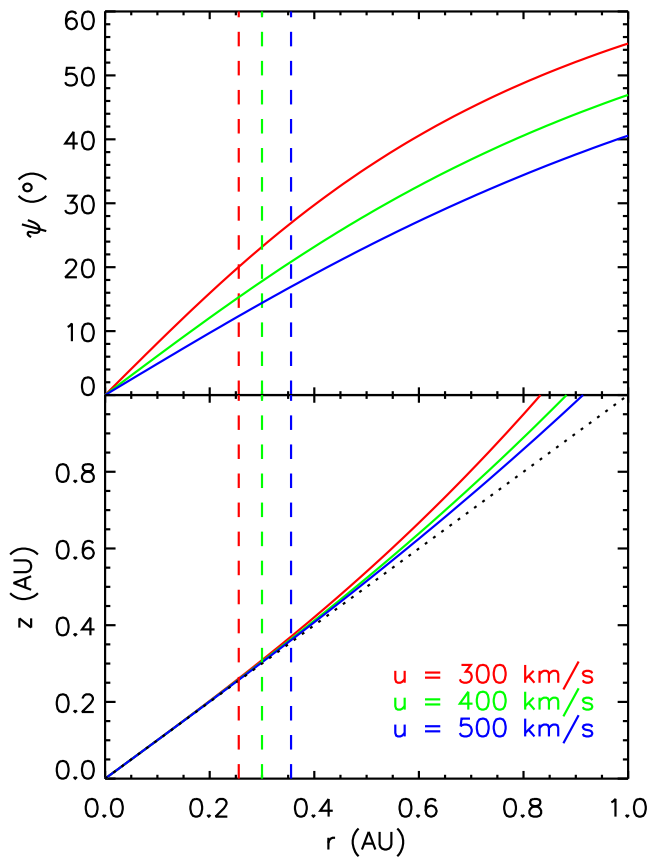
FIG. 2: $\psi(r)$ angle (*top*) and distance along the field line, z, (*bottom*) as a function of radial distance r from the Sun. We assumed different values of the solar wind speed (300 km/s, 400 km/s and 500 km/s).

radial field in which we assume $z \sim r$ because $|z - r| < 5 \times 10^{-3}$. For each solar wind speed analyzed (300 km/s, 400 km/s and 500 km/s), the boundary is located at 0.25 AU, 0.30 AU and 0.35 AU, respectively (see vertical lines in Fig. 2), that is, the boundary is closer to the Sun for slower solar wind speeds. In addition, we can also see that at the *SolO* and *SPP* perihelia (0.30 and 0.05 AU, respectively), $z \sim r$, especially close to the Sun (< 0.05 AU) and for high solar wind speeds.

B.   Focusing effect

In a slowly varying magnetic field, the first adiabatic invariant remains constant (Eq. 2). This implies that the particle pitch angle at a given location is related to its initial state (pitch angle and location) by the following equation

$$\mu(r) = \pm\sqrt{1 - \frac{B(r)}{B_0}(1 - \mu_0^2)} \qquad (7)$$

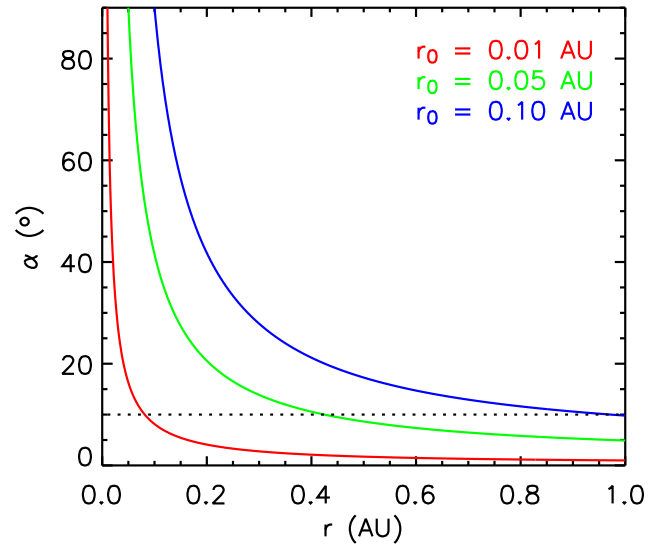where the particle is initially at position r_0 with pitch angle cosine μ_0 [8].

FIG. 3: Pitch angle α at different radial distances from the Sun assuming $\alpha_0 = 90°$ at different source position $r_0 = [0, 0.01, 0.05, 0.1]$ AU. We assumed a solar wind speed of 400 km/s.

Eq. 7 shows that the final value of the pitch-angle cosine depends on the value of μ_0 and the ratio between magnetic field intensities.

Fig. 3 shows the expected particle pitch angle at different radial distances from the Sun assuming an initial pitch angle equal to 90° and different source positions for a solar wind speed of 400 km/s. It can be seen that if the particle is released close to the Sun (0.01 AU), the PAD at 0.08 AU is a beam only $\sim 10°$ wide. On the other hand, if the source position is far from the Sun, for example at 0.10 AU, the pitch angle decreases more slowly and it reaches 10° at 1 AU instead. Table I lists the pitch-angle values expected at 1 AU, 0.3 AU and 0.05 AU assuming a solar wind speed of 400 km/s and several source positions.

We computed the results shown in Fig. 3 for several solar wind speeds. The differences are found to be very small in all cases: they are less than 1° assuming $u = 300$ km/s or $u = 500$ km/s.

C.   Transit time along the field line

The differential distance along the particle's full trajectory ds can be expressed by $ds = vdt$, which can be expressed by a function of the differential distance along the field line

$$ds = \frac{1}{\mu}dz \qquad (8)$$

The time elapsed in the propagation is $\Delta t(r, \mu; r_0, \mu_0) = \frac{\Delta s(r, \mu; r_0, \mu_0)}{v}$, where $\Delta s(r, \mu; r_0, \mu_0)$ is the trajectory path length between the initial position

r_0	Pitch angle, α (°)				$v\Delta t$ (AU)
(AU)	r = 0.05 AU	r = 0.3 AU	r = 1 AU	r ≃ 0.15 AU	r ≃ 0.15 AU
0.01	15	3	1	6	0.144
0.05	90	14	5	28	0.136
0.10		28	10	61	0.105

TABLE I: Pitch angle expected for different source positions, r_0 and different locations of the observers. For z = 0.15 AU (r *simeq* 0.15) the elapsed time v∆t is listed. We assumed $\alpha_0 = 90°$ and solar wind speed equal to 400 km/s.
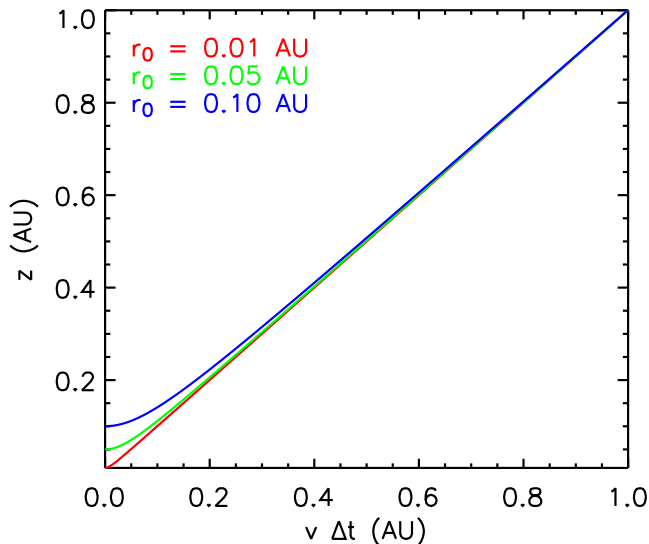

FIG. 4: $v\Delta t$ as a function of z assuming different source position, $r_0 = [0, 0.01, 0.05, 0.1]$ AU, as above and initial pitch angle 90°.

FIG. 5: Pitch angle as a function of the source position, r_0, assuming an initial pitch angle of 90° and a solar wind speed of 400 km/s for different observer positions.

r_0 (where the particle has pitch angle cosine equal to μ_0) and r, and it is given by (see [8] for complete equations)

$$\Delta s(r, \mu; r_0, \mu_0) = \mid s(r, \mu; r_0, \mu_0) - s(r_0, \mu_0; r_0, \mu_0) \mid \quad (9)$$

With these equations we computed the elapsed "time" (vt) as a function of the distance along the field line z (see Fig. 4). For particles released very close to the Sun ($r_0 = 0.01$ AU) the equation of motion is a line. This means that for these particles the acceleration process along the field is very short (the focusing effect decreases the particle pitch angle fast close to the Sun). For outer values of the source position, the particle trajectory is not a line inside 0.4 AU. This is related to the fact that the focusing effect is weaker outer in the corona and the particle pitch angle decreases more slowly. In other words, as the pitch angle decreases, $v_{\parallel}$ increases (see Eq. 1) which produces a faster translation along the field line. When $\alpha \sim 0°$ the particle moves at constant speed along the field line, but before that its $v_{\parallel}$ is gradually increasing (faster the closer to the Sun it was released).

For a fixed distance along the field line, the particles coming from different source positions reach the observer at different times (Fig. 4). For a fixed distance along the
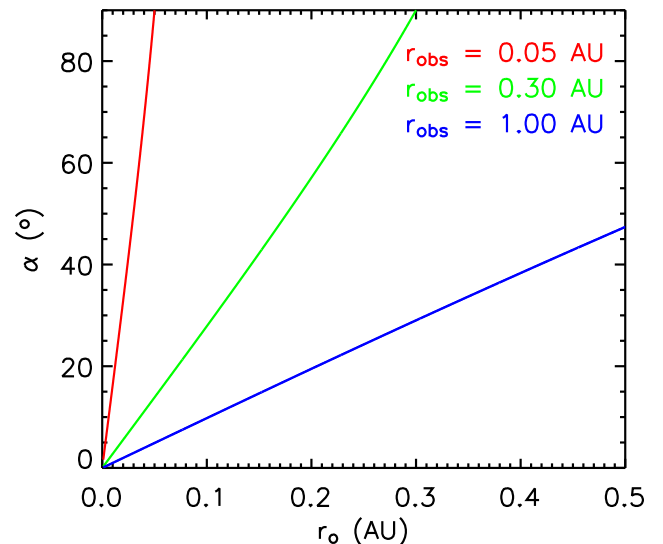
field line of e.g. $z_1 = 0.15$ AU, the transit time is shorter and the PAD is broader for particles released outer from the Sun (see Table I).

III.   MOVING SOURCE PARAMETRIZATION

In this section we study the focusing cone produced by sources at different locations in the corona. Fig. 5 and Table II show the results. For a given source location, the focusing cone is broader the closer to the Sun the observer is. This is expected, as particles propagating further out do suffer more focusing. This means that in the inner heliosphere (< 0.5 AU) we expect broader PADs than at 1 AU for a fixed source position. The closer to the Sun the source is, the narrower the PADs (the smaller the focusing cone) expected in different regions of the heliosphere. For more external source locations, the observer and the source are closer and this translates into broader PADs close to the Sun than at 1 AU. For example, a source located at $10R_{\odot}$ releasing particles with pitch angles [0,90°] would produce a focusing cone at 0.05 AU of 80° (i.e. particles with pitch angles from 0 to 80° would be ob-

$r_{\mathrm{obs}} = 0.05$ AU				$r_{\mathrm{obs}} = 0.3$ AU				$r_{\mathrm{obs}} = 1.0$ AU			
Source location	α	$v\Delta t$		Source location	α	$v\Delta t$		Source location	α	$v\Delta t$	
(AU)	($R_\odot$)	(°)	(AU)	(AU)	($R_\odot$)	(°)	(AU)	(AU)	($R_\odot$)	(°)	(AU)
0.01	2.2	10	0.050	0.04	8.6	10	0.303	0.102	21.5	10	1.168
0.02	4.3	30	0.047	0.11	25.8	30	0.287	0.31	66.6	30	1.168
0.03	6.5	50	0.040	0.18	38.7	50	0.252	0.53	113.9	50	1.137
0.04	8.6	70	0.029	0.24	51.6	70	0.189	0.76	163.4	70	0.976
0.05	10.7	89	0.006	0.30	64.5	89	0.043	0.99	212.8	89	0.263

TABLE II: Pitch angle cone and elapsed "time" expected for several source locations at three different radial distances ($r_{\mathrm{obs}} = 0.05$ AU, 0.30 AU and 1.00 AU).

served). On the other hand, the focusing cone would be of only 10° at 0.3 AU and of 4.5° at 1 AU. Thus, broader PADs are expected close to the Sun due to the release of particles from outer sources. CMEs can produce coronal shocks that would act as moving particle sources. In this case, an observer in the inner heliosphere would observe a superposition of PADs produced by the particles released at different source locations due to the movement of the CME. Earlier PADs would be more beamed than later PADs.

IV. DISCUSSION AND SUMMARY

PADs measured in different regions of the heliosphere are essential to determine the processes of particle release at the Sun and understand the effects of particle interplanetary propagation.

We studied the main characteristics of the IMF described by a Archimedean spiral and we verified that close to the Sun the magnetic field lines are almost radial, especially at *SolO* and *SPP* perihelia. Under the assumption of scatter-free transport, we obtained that for a fixed source position the angular distribution of particles is expected to be more beamed for larger radial distances. This is due to the fact that the magnetic field intensity decreases rapidly with distance. On the other hand, the angular distribution is expected to be broader at a fixed radial distance from the Sun for outer source lo-

cations. Moreover we found that the equation of motion for particles released close to the Sun follow a line, while particles released from an external source suffer some acceleration process along the field. This is linked with the fact that the focusing effect is weaker outer in the corona and the pitch angle decreases more slowly for particles released outer in the corona. For a fixed distance along the field line, particles released outer will arrive earlier. For an observer close to the Sun, this effect will be more important.

An analysis of the focusing cone expected in different regions of the heliosphere due to different source locations indicates that we should expect broader PADs in the inner heliosphere than at 1 AU. This is due to the fact that particles observed close to the Sun suffer less focusing than at 1 AU. In addition, outer particle sources produce broader PADs due to the weaker focusing effect.

[1] Agueda, N., Klein, K.-L., Vilmer, N., et al. 2014, A&A, 570, A5
[2] Krucker, S., Larson, D. E., Lin, R. P., & Thompson, B. J. 1999, Astrophys. J. , 519, 864
[3] Reames, D. V. 1999, Space Sci. Rev., 90, 413
[4] Parker, E. N. 1958, Astrophys. J. , 128, 664
[5] Kallenrode, M.-B., & Wibberenz, G. 1990, Int. Cosmic Ray Conf., 5, 229
[6] Müller, D., Marsden, R. G., St. Cyr, O. C., & Gilbert, H. R. 2013, Sol. Phys., 285, 25
[7] Fox, N. J., Velli, M. C., Bale, S. D., et al. 2015, Space Sci. Rev.,
[8] Agueda, N. 2008, Ph.D. Thesis, Universitat de Barcelona
[9] Kunow, H., Wibberenz, G., Green, G., Müller-Mellin, R., & Kallenrode, M.-B. 1991, Physics of the Inner Heliosphere II, 152
[10] Vainio, R., Koskinen, H., Heber, B., Agueda, N. & Kilpua, E. 2013, Lecture notes on Solar eruptions and space environment, http://www.sepserver.eu/sepserver/asset/e7ad3d76-fc74-4387-8fa7-a3ca356363fa/D7.2.pdf